

A Practical Sparse Approximation for Real Time Recurrent Learning

Jacob Menick* DeepMind University College London	Erich Elsen* DeepMind	Utku Evci Google
Simon Osindero DeepMind	Karen Simonyan DeepMind	Alex Graves DeepMind

{jmenick, eriche, evcu, osindero, simonyan, graves}@google.com

Abstract

Current methods for training recurrent neural networks are based on backpropagation through time, which requires storing a complete history of network states, and prohibits updating the weights ‘online’ (after every timestep). Real Time Recurrent Learning (RTRL) eliminates the need for history storage and allows for online weight updates, but does so at the expense of computational costs that are quartic in the state size. This renders RTRL training intractable for all but the smallest networks, even ones that are made highly sparse. We introduce the Sparse n -step Approximation (SnAp) to the RTRL influence matrix, which only keeps entries that are nonzero within n steps of the recurrent core. SnAp with $n = 1$ is no more expensive than backpropagation, and we find that it substantially outperforms other RTRL approximations with comparable costs such as Unbiased Online Recurrent Optimization. For highly sparse networks, SnAp with $n = 2$ remains tractable and can outperform backpropagation through time in terms of learning speed when updates are done online. SnAp becomes equivalent to RTRL when n is large.

1 Introduction

Recurrent neural networks (RNNs) have been successfully applied to a wide range of sequence learning tasks, including text-to-speech [19], language modeling [7], automatic speech recognition [1], translation [4] and reinforcement learning [11]. RNNs have greatly benefited from advances in computational hardware, dataset sizes, and model architectures. However, the algorithm used to compute their gradients remains unchanged: Back-Propagation Through Time (BPTT). The key limitation of BPTT is that the entire state history must be stored, meaning that the memory cost grows linearly with the sequence length. For sequences too long to fit in memory, as often occurs in domains such as language modelling or long reinforcement learning episodes, truncated BPTT (TBPTT) [30] can be used. Unfortunately the truncation length used by TBPTT also limits the duration over which temporal structure can be reliably learned.

*These authors contributed equally to this work

Forward-mode differentiation, or Real-Time Recurrent Learning (RTRL) as it is called when applied to RNNs [29], solves some of these problems. It doesn't require storage of any past network states, can theoretically learn dependencies of any length and can be used to update parameters at any desired frequency, including every step (i.e. fully online). However, its fixed storage requirements are $O(k \cdot |\theta|)$, where k is the state size and $|\theta|$ is the number of parameters θ in the core. Perhaps even more daunting, the computation it requires is $O(k^2 \cdot |\theta|)$. This makes it impractical for even modestly sized networks. The advantages of RTRL have led to a search for more efficient approximations that retain its desirable properties, whilst reducing its computational and memory costs. One recent line of work introduces unbiased, but noisy approximations to the influence update. Unbiased Online Recurrent Optimization (UORO) [28] is an approximation with the same cost as TBPTT – $O(|\theta|)$ – however its gradient estimate is severely noisy [6] and its performance has in practice proved worse than TBPTT [23]. Less noisy approximations with better accuracy on a variety of problems include both Kronecker Factored RTRL (KF-RTRL) [23] and Optimal Kronecker-Sum Approximation (OK) [2]. However, both increase the computational costs to $O(k^3)$.

The last few years have also seen a resurgence of interest in sparse neural networks – both their properties [13] and new methods for training them [12]. A number of works have noted their theoretical and practical efficiency gains over dense networks [31, 25, 9]. Of particular interest is the finding that scaling the state size of an RNN while keeping the number of parameters constant leads to increased performance [19].

In this work we introduce a new sparse approximation to the RTRL influence matrix. The approximation is biased but not stochastic. Rather than tracking the full influence matrix, we propose to track only the influence of a parameter on neurons that are affected by it within n steps of the RNN. The algorithm is strictly less biased but more expensive as n increases. The cost of the algorithm is controlled by n and the amount of sparsity in the Jacobian of the recurrent cell. Larger n can be coupled with concomitantly higher sparsity to keep the cost fixed. The approximation approaches full RTRL as n increases. Our contributions are as follows:

- We propose SnAp – a practical approximation to RTRL, which is applicable to both dense and sparse RNNs, and is based on the sparsification of the influence matrix.
- We show that parameter sparsity in RNNs reduces the costs of RTRL in general and SnAp in particular.
- We carry out experiments on both real-world and synthetic tasks, and demonstrate that the SnAp approximation: (1) works well for language modeling compared to the exact unapproximated gradient; (2) admits learning long-term dependencies on a synthetic copy task and (3) can learn faster than BPTT when run fully online.

2 Background

We consider recurrent networks whose dynamics are governed by $h_t = f_\theta(h_{t-1}, x_t)$ where $h_t \in \mathbb{R}^k$ is the state, $x_t \in \mathbb{R}^a$ is an input, and $\theta \in \mathbb{R}^p$ are the network parameters. It is assumed that at each step $t \in \{1, \dots, T\}$, the state is mapped to an output $y_t = g_\phi(h_t)$, and the network receives a loss $\mathcal{L}_t(y_t, y_t^*)$. The system optimizes the total loss $\mathcal{L} = \sum_t \mathcal{L}_t$ with respect to parameters θ by following the gradient $\nabla_\theta \mathcal{L}$. The standard way to compute this gradient is BPTT – running backpropagation on the computation graph “unrolled in time” over a number of steps T :

$$\nabla_\theta \mathcal{L} = \sum_{t=1}^T \frac{\partial \mathcal{L}}{\partial h_t} \frac{\partial h_t}{\partial \theta_t} = \sum_{t=1}^T \left(\frac{\partial \mathcal{L}}{\partial h_{t+1}} \frac{\partial h_{t+1}}{\partial h_t} + \frac{\partial \mathcal{L}_t}{\partial h_t} \right) \frac{\partial h_t}{\partial \theta_t} \quad (1)$$

The recursive expansion $\frac{\partial \mathcal{L}}{\partial h_t} = \frac{\partial \mathcal{L}}{\partial h_{t+1}} \frac{\partial h_{t+1}}{\partial h_t} + \frac{\partial \mathcal{L}_t}{\partial h_t}$ is the backpropagation rule. The slightly nonstandard notation θ_t

refers to the copy of the parameters used at time t , but the weights are shared for all timesteps and the gradient adds over all copies.

2.1 Real Time Recurrent Learning (RTRL)

Real Time Recurrent Learning [29] computes the gradient as:

$$\nabla_{\theta} \mathcal{L} = \sum_{t=1}^T \frac{\partial \mathcal{L}_t}{\partial h_t} \frac{\partial h_t}{\partial \theta} = \sum_{t=1}^T \frac{\partial \mathcal{L}_t}{\partial h_t} \left(\frac{\partial h_t}{\partial \theta_t} + \frac{\partial h_t}{\partial h_{t-1}} \frac{\partial h_{t-1}}{\partial \theta} \right) \quad (2)$$

This can be viewed as an iterative algorithm, updating $\frac{\partial h_t}{\partial \theta}$ from the intermediate quantity $\frac{\partial h_{t-1}}{\partial \theta}$. To simplify equation 2 we introduce the following notation: have $J_t := \frac{\partial h_t}{\partial \theta}$, $I_t := \frac{\partial h_t}{\partial \theta_t}$ and $D_t := \frac{\partial h_t}{\partial h_{t-1}}$. J stands for ‘‘Jacobian’’, I for ‘‘immediate Jacobian’’, and D for ‘‘dynamics’’. We sometimes refer to J as the ‘‘influence matrix’’. The recursion can be rewritten $J_t = I_t + D_t J_{t-1}$.

Cost analysis J_t is a matrix in $\mathbb{R}^{k \times |\theta|}$, which can be on the order of gigabytes for even modestly sized RNNs. Furthermore, performing the operation $D_t J_{t-1}$ involves multiplying a $k \times k$ matrix by a $k \times |\theta|$ matrix each timestep. That requires $|\theta|$ times more computation than the forward pass of the RNN core. To make explicit just how expensive RTRL is – this is a factor of roughly one million for a vanilla RNN with 1000 hidden units.

2.2 Truncated RTRL and stale Jacobians

In analogy to Truncated BPTT, one can consider performing a gradient update partway through a training sequence (at time t) but still passing forward a stale state *and* a stale influence Jacobian J_t rather than resetting both to zero after the update. This enables more frequent weight updating at the cost of a staleness bias. The Jacobian J_t becomes ‘‘stale’’ because it tracks the sensitivity of the state to old parameters. Experiments (section 5.2) show that this tradeoff can be favourable toward more frequent updates in terms of data efficiency. In fact, much of the RTRL literature assumes that the parameters are updated at every step t (‘‘fully online’’) and that the influence Jacobian is never reset, at least until the start of a new sequence.

2.3 Sparsity in RNNs

One of the early explorations of sparsity in the parameters of RNNs (i.e. many entries of θ are exactly zero) was Ström [27], where one-shot pruning based on weight magnitude with subsequent retraining was employed in a speech recognition task. The current standard approach to inducing sparsity in RNNs [31] remains similar, except that magnitude based pruning happens slowly over the course of training so that no retraining is required.

Kalchbrenner et al. [19] discovered a powerful property of sparse RNNs in the course of investigating them for text-to-speech – for a constant parameter and flop budget sparser RNNs have *more* capacity per parameter than dense ones. This property has so far only been shown to hold when the sparsity pattern is adapted during training (in this case, with pruning). Note that parameter parity is achieved by simultaneously increasing the RNN state size and the degree of sparsity. This suggests that training large sparse RNNs could yield powerful sequence models, but the memory required to store the history of (now much larger) states required for BPTT becomes prohibitive for long sequences.

3 The Sparse n-Step Approximation (SnAp)

Our main contribution in this work is the development of an approximation to RTRL called the Sparse n-Step Approximation (SnAp) which reduces RTRL’s computational requirements substantially.

SnAp imposes sparsity on J even though it is in general dense. We choose the sparsity pattern to be the locations that are non-zero after n steps of the RNN (Figure 1). We also choose to use the same pattern for all steps, though this is not a requirement. This means that the sparsity pattern of J_t is known and can be used to reduce the amount of computation in the product $D_t J_{t-1}$. See Figure 2 for a visualization of the process. The costs of the resulting methods are compared in Table 1. We note an alternative strategy would be to perform the full multiplication of $D_t J_{t-1}$ and then only keep the top- k values. This would reduce the bias of the approximation but increase its cost.

More formally, we adopt the following approximation for all t :

$$(J_t)_{ij} \approx \begin{cases} (J_t)_{ij} & \text{if } (\theta_t)_j \text{ influences hidden unit } (h_{t+n})_i \\ 0 & \text{otherwise} \end{cases}$$

3.1 Sparse One-Step Approximation (SnAp-1)

Even for a fully dense RNN, each parameter will in the usual case only immediately influence the single hidden unit it is directly connected to. This means that the immediate Jacobian I_t tends to be extremely sparse. For example, a Vanilla RNN will have only one nonzero element per column, which is a sparsity level of $\frac{k-1}{k}$. Storing only the nonzero elements of I_t already saves a significant amount of memory without making any approximations; I_t is the same shape as the daunting J_t matrix whereas the nonzero values are the same size as θ .

I_t can become more dense in architectures (such as GRU and LSTM) which involve the composition of parameterised layers within a single core step (see section 3.3 for an in-depth discussion of the effect of gating architectures on Jacobian sparsity). In the Sparse One-Step Approximation, we only keep entries in J_t if they are nonzero in I_t . After just two RNN steps, a given parameter has influenced every unit of the state through its intermediate influence on other units. Thus only SnAp with $n = 1$ is efficient for dense RNNs because $n > 1$ does not result in any sparsity in J , i.e.: for dense networks SnAp-2 already reduces to full RTRL. (N.b.: SnAp-1 is also applicable to sparse networks.) Figure 1 depicts the sparse structure of the influence of a parameter for both sparse and fully dense cases.

SnAp-1 is effectively diagonal, in the sense that the effect of parameter j on hidden unit i is maintained throughout time, but ignoring the indirect effect of parameter j on unit i via paths through other units i' . More formally, it is useful to define $u(j)$ as the one component in the state h_t connected directly to the parameter j (which has at the other end of the connection some other entry i' within h_{t-1} or x_t). Let $i = u(j)$. The imposition of the one-step sparsity pattern means only the entry in row i will be kept for column j in J_t . Inspecting the update for this particular entry, we have

$$(J_t)_{ij} = (I_t)_{ij} + \sum_{m=1}^n (D_t)_{im} (J_{t-1})_{mj} = (I_t)_{ij} + (D_t)_{ii} (J_{t-1})_{ij} \tag{3}$$

The equality follows from the assumption that $(J_{t-1})_{mj} = 0$ if $m \neq i$. Diagonal entries in D_t are thus crucial for this approximation to be expressive, such as those arising from skip connections.

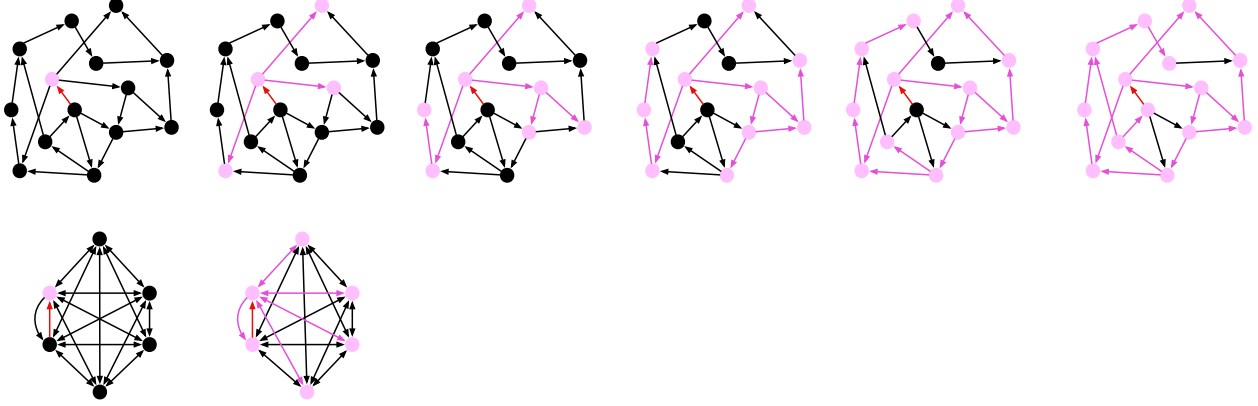


Figure 1: SnAp in dense (bottom) and sparse (top) graphs: As the figure proceeds to the right we propagate the influence of the red connection i on the nodes j of the graph through further RNN steps. Nodes are colored in pink if they are influenced on or before that step. The entry $J_{i,j}$ is kept if node j is colored pink, but all other entries in row i are set to zero. When $n = 1$ in both cases only one node is influenced. In the dense case the red connection influences all nodes when $n >= 2$.

3.2 Optimizations for full RTRL with sparse networks

When the RNN is sparse, the costs of even full (unapproximated) RTRL can be alleviated to a surprising extent; we save computation proportional to a factor of the sparsity *squared*. Assume a proportion s of the entries in both θ and D_t are equal to zero and refer to this number as “the level of sparsity in the RNN”. For convenience, $d := 1 - s$. With a Vanilla RNN, this correspondence between parameter sparsity and dynamics sparsity holds exactly. For popular gating architectures such as GRU and LSTM the relationship is more complicated so we include empirical measurements of the computational cost in FLOPS (Table 3) in addition to the theoretical calculations here. More complex recurrent architectures involving attention [26] would require an independent mechanism for inducing sparsity in D_t ; we leave this direction to future work and assume in the remainder of this derivation that sparsity in θ corresponds to sparsity in D_t .

If the sparsity level of θ is s , then so is the sparsity in J because the columns corresponding to parameters which are clamped to zero have no effect on the gradient computation. We may extract the columns of J containing nonzero parameters into a new dense matrix \tilde{J} used in place of J everywhere with no effect on the gradient computation. We make the same optimization for I_t and use the dense matrix \tilde{I}_t in its place, leaving us with the update rule (depicted in Figure 2) :

$$\tilde{J}_t = \tilde{I}_t + D_t \tilde{J}_{t-1} \quad (4)$$

These optimizations taken together reduce the storage requirements by $\frac{1}{d}$ (because \tilde{J} is d times the size of J) and the computational requirements by $\frac{1}{d^2}$ because D_t in the sparse matrix multiplication $D_t \tilde{J}_{t-1}$ has density d , saving us an extra factor of $\frac{1}{d}$.

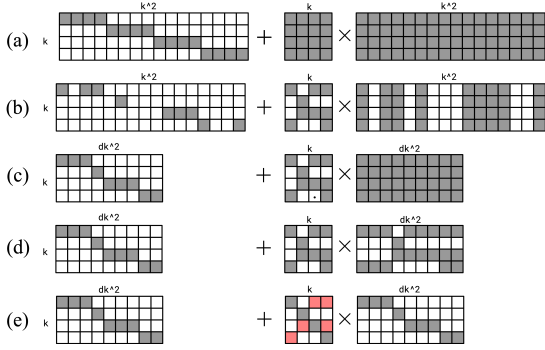


Figure 2: Depiction of RTRL, RTRL with sparsity and SnAp. White indicates zeros. (a) $I_t + D_t J_{t-1}$ (b) $I_t + D_t J_{t-1}$ when W is sparse (c) $\tilde{I}_t + D_t \tilde{J}_{t-1}$ (d) SnAp-2 (e) SnAp-1. Rose colored squares are non-zero in D_t but not used in updating J_t .

Method	memory	time per step
BPTT	$Tk + p$	$k^2 + p$
UORO	$k + p$	$k^2 + p$
RTRL	$k + kp$	$k^2 + k^2 p$
Sparse BPTT	$Tk + dp$	$d(k^2 + p)$
Sparse RTRL	$k + dkp$	$d(k^2 + dk^2 p)$
SnAp-1	$k + dp$	$d(k^2 + p)$
SnAp-2	$k + d^2 kp$	$d(k^2 + d^2 k^2 p)$

Table 1: Computational costs of gradient calculation methods for dense and sparse RNNs. Below T refers to the sequence length, k the number of hidden units, p the number of recurrent parameters, s the level of sparsity, and $d = 1 - s$.

3.3 Sparse N Step Approximation (SnAp- N)

Even when D_t is sparse, the computation “graph” linking nodes (neurons) in the hidden state over time should still be connected, meaning that \tilde{J} eventually becomes fully dense because after enough iterations every (non-zero) parameter will have influenced every hidden unit in the state. Thus sparse approximations are still available in this setting and indeed required to obtain an efficient algorithm. For sparse RNNs, SnAp simply imposes additional sparsity on \tilde{J}_t rather than J_t . SnAp- N for $N > 1$ is both strictly less biased and strictly more expensive, but its costs can be reduced by increasing the degree s of sparsity in the RNN. SnAp-2 is comparable with UORO and SnAp-1 if the sparsity of the RNN is increased so that $d < n^{-\frac{2}{3}}$, e.g. 99% or higher sparsity for a 1000-unit Vanilla RNN. If this level of sparsity is surprising, the reader is encouraged to see our experiments in section 5.1.2.

Jacobian Sparsity of GRUs and LSTMs

Unlike vanilla RNNs whose dynamics Jacobian D_t has sparsity exactly equal to the sparsity of the weight matrix, GRUs and LSTMs have inter-cell interactions which increase the Jacobians’ density. In particular, the choice of GRU variant can have a very large impact on the increase in density. This is relevant to the “dynamics” jacobian D_t and the parameter jacobians I_t and J_t .

Consider a standard formulation of LSTM.

$$\begin{aligned}
 i_t &= \sigma(W_{ii}x_t + W_{hi}h_{t-1} + b_i) \\
 f_t &= \sigma(W_{if}x_t + W_{hf}h_{t-1} + b_f) \\
 o_t &= \sigma(W_{io}x_t + W_{ho}h_{t-1} + b_o) \\
 g_t &= \phi(W_{ig}x_t + W_{hg}h_{t-1} + b_g) \\
 c_t &= f_t \odot c_{t-1} + i_t \odot g_t \\
 h_t &= o_t \odot \phi(c_t)
 \end{aligned} \tag{5}$$

Looking at LSTM’s update equations, we can see that an individual parameter (W, b) will only directly affect one entry in each gate (i_t, f_t, o_t) and the candidate cell g_t . These in turn produce the next cell c_t and next hidden state h_t with element-wise operations (σ is the sigmoid function applied element-wise and ϕ is usually hyperbolic tangent). In this case Figure 1 is an accurate depiction of the propagation of influence of a parameter as the RNN is stepped.

However, for a GRU there are multiple variants in which a parameter or hidden unit can influence many more units of the next state. The original variant [5] is as follows:

$$\begin{aligned}
 z_t &= \sigma(W_{iz}x_t + W_{hz}h_{t-1} + b_z) \\
 r_t &= \sigma(W_{ir}x_t + W_{hr}h_{t-1} + b_r) \\
 a_t &= \phi(W_{ia}x_t + W_{ha}(r_t \odot h_{t-1}) + b_a) \\
 h_t &= (1 - z_t) \odot h_{t-1} + z_t \odot a_t
 \end{aligned} \tag{6}$$

For our purposes the main thing to note is that the parameters influencing r_t further influence every unit of a_t because of the matrix multiplication by W_{ha} . They therefore influence every unit of h_t within one recurrent step, which means that the dynamics jacobian D_t is fully dense and the immediate parameter jacobian I_t for W_{ir} , W_{hr} , and b_r are all fully dense as well.

An alternative formulation which was popularized by Engel [10], and also used in the CuDNN library from NVIDIA is given by:

$$\begin{aligned}
 z_t &= \sigma(W_{iz}x_t + W_{hz}h_{t-1} + b_z) \\
 r_t &= \sigma(W_{ir}x_t + W_{hr}h_{t-1} + b_r) \\
 a_t &= \phi(W_{ia}x_t + r_t \odot W_{ha}h_{t-1} + b_a) \\
 h_t &= (1 - z_t) \odot h_{t-1} + z_t \odot a_t
 \end{aligned} \tag{7}$$

The second variant has moved the reset gate after the matrix multiplication, thus avoiding the composition of parameterized linear maps within a single RNN step. As the modeling performance of the two variants has been shown to be largely the same, but the second variant is faster and results in sparser D_t and I_t , we adopt the second variant throughout this paper.

4 Related Work

SnAp-1 is actually similar to the original algorithm used to train LSTM [18], which employed forward-mode differentiation to maintain the sensitivity to each parameter of a single cell unit, over all time. This exposition was expressed in terms coupled to the LSTM architecture whereas our formulation is general. Random Feedback Local Online [24] (RFLO) amounts to accumulating I_t terms in equation 4 whilst ignoring the product $D_t J_{t-1}$. It admits an efficient implementation through operating on \tilde{I}_t as in section 3.2 but is strictly more biased than the approximations considered in this work and performs worse in our experiments. As mentioned in section 1, stochastic approximations to the influence matrix are an alternative to the methods developed in our work, but suffer from noise in the gradient estimator [6]. A fruitful line of research focuses on reducing this noise [6], [23], [2].

It is possible to reduce the storage requirements of TBPTT using a technique known as “gradient checkpointing” or “rematerialization”. This reduces the memory requirements of backpropagation by recomputing states rather than storing them. First introduced in Griewank and Walther [15] and later applied specifically to RNNs in Gruslys et al.

[16], these methods are not compatible with the fully online setting where T may be arbitrarily large as even the optimally small amount of re-computation can be prohibitive. For reasonably sized T , however, rematerialization is a straightforward and effective way to reduce the memory requirements of TBPTT, especially if the forward pass can be computed quickly.

5 Experiments

We include experimental results on the real world language-modelling task WikiText103 [22] and the synthetic ‘Copy’ task [14] of simply repeating an observed binary string. Whilst the first is important for demonstrating that our methods can be used for real, practical problems, language modelling doesn’t directly measure a model’s ability to learn structure that spans long time horizons. The Copy task, however, allows us to parameterize exactly the temporal distance over which structure is present in the data. In terms of, respectively, task complexity and RNN state size (up to 1024) these investigations are considerably more “large-scale” than much of the RTRL literature.

5.1 WikiText103

All of our WikiText103 experiments tokenize at the character (byte) level and use SGD to optimize the log-likelihood of the data. We use the Adam optimizer [20] with $\beta_1 = 0.9$, $\beta_2 = 0.999$, and $\epsilon = 1e^{-8}$. We train on randomly cropped sequences of length 128 sampled uniformly with replacement and do not propagate state across the end-of-sequence boundary (i.e. no truncation). Results are reported on the standard validation set.

5.1.1 Language Modelling with dense RNNs: SnAp-1

In this section, we refrain from performing a weight update until the end of a training sequence (see section 2.2) so that BPTT is the gold standard benchmark for performance, assuming the gradient is the optimal descent direction. The architecture is a Gated Recurrent Unit (GRU) network [5] with 128 recurrent units and a one-layer readout MLP mapping to 1024 hidden units before the final 256-unit softmax layer. Learning curves in Figure 3 (Left) show that SnAp-1 outperforms RFLO and UORO, and that in this setting UORO fails to match the surprisingly strong baseline of not training the recurrent parameters at all and instead leaving them at their randomly initialized value.

5.1.2 Language Modeling with Sparse RNNs: SnAp-1 and SnAp-2

Here we use the same architecture as in section 5.1.1, except that we introduce 75% sparsity into the weights of the GRU, in particular the weight matrices (more sparsity levels are considered in later experiments). Biases are always kept fully dense. In order to induce sparsity, we generate a sparsity pattern uniformly at random and fix it throughout training. As would be expected because it is strictly less biased, Figure 3 (Right) shows that SnAp-2 outperforms SnAp-1 but only slightly. Furthermore, both closely match the (gold-standard) accuracy of a model trained with BPTT. Table 3 shows that SnAp-2 actually costs about 600x more FLOPs than BPTT/SnAp-1 at 75% sparsity, but higher sparsity substantially reduces FLOPs. It’s unclear exactly how the cost compares to UORO, which though $O(|\theta|)$ does have constant factors required for e.g. random number generation, and additional overheads when approximations use rank higher than one.

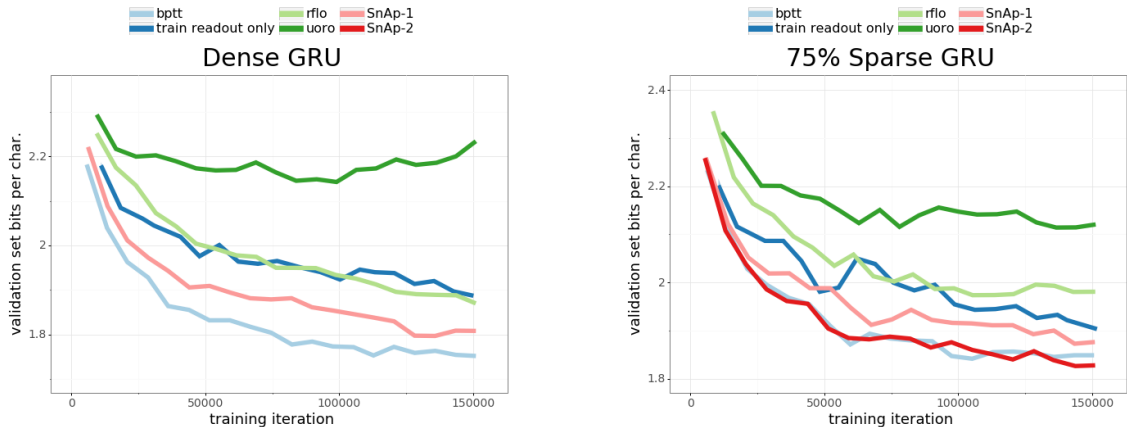


Figure 3: **Left:** Comparing various RTRL approximations based upon their ability to train a dense GRU network to do character-level language modelling. On the y-axis is Negative Log Likelihood. **Right:** Same as left with 75% parameter-sparsity.

Sparsity Strategy Our experiments do not use state-of-the-art strategies for inducing sparsity because there is no such strategy compatible with SnAp at the time of writing. The requirement of a dense gradient in Evci et al. [12] and Zhu and Gupta [31] prevents the use of the optimization in Equation 4, which is strictly necessary to fit the RTRL training computations on accelerators without running out of memory.

To further motivate the development of sparse training strategies that do not require dense gradients, we show that larger sparser networks trained with BPTT and magnitude pruning monotonically outperform their denser counterparts in language modelling, when holding the number of parameters constant. This provides more evidence for the scaling law observed in Kalchbrenner et al. [19].

The experimental setup is identical to the previous section except that all networks are trained with full BPTT. To hold the number of parameters constant, we start with a fully dense 128-unit GRU. We make the weight matrices 75% sparse when the network has 256 units, 93.8% sparse when the network has 512 units, 98.4% when the network has 1024 units, and so on. The sparsest network considered has 4096 units and over 99.9% sparsity, and performed the best. Indeed it performed better than a dense network with 6.25x as many parameters (Figure 4). Pruning decisions are made on the basis of absolute value every 1000 steps, and the final sparsity is reached after 350,000 training steps.

5.2 Copy Task

Our experiments on the Copy task aim to investigate the ability of the proposed sparse RTRL approximations to learn about long-term temporal structure. We follow [23] and adopt a curriculum-learning approach over the length L of sequences to be copied, starting with $L = 1$. When the average bits per character of a training minibatch drops below 0.15, we increment L by one. We sample the length of target sequences uniformly between $[\max(L - 5, 1), L]$ as in previous work. After some number of training steps, we compare algorithms on the basis of the level of L they have reached because a model which has reached a greater L has more rapidly learned how to capture structure over a time horizon of L steps¹. We measure performance versus ‘data-time’, i.e. we give each algorithm a time budget in units of the cumulative number of tokens seen throughout training. A consequence of this scheme is that full BPTT is no

¹actually $2 * L + 2$ because of start/end flags and because the observation/target are presented in sequence

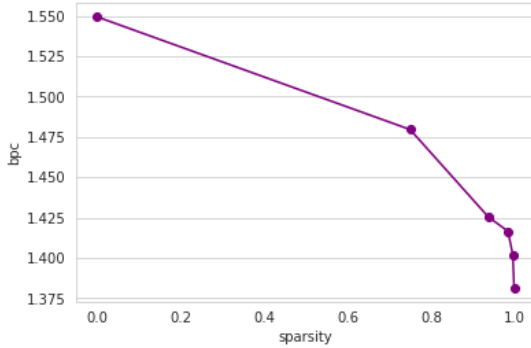


Figure 4: BPC vs Sparsity for Constant Parameter Count. Shows the same results as Table 2. The biggest, sparsest GRU performs better than a dense network with 6.25x as many (nonzero) parameters.

units	bpc	θ sparsity	$ \theta $
base	1.55	0%	1x
2x	1.48	75%	1x
4x	1.43	93.75%	1x
8x	1.42	98.4%	1x
16x	1.40	99.6%	1x
32x	1.38	99.9%	1x
2.5x	1.39	0%	6.25x

Table 2: Final performance of sparse Wiki-Text103 language modeling GRU networks trained with progressive pruning. Each row represents a single training run. The ‘bpc’ column gives the validation set negative log-likelihood in units of bits per character. The $|\theta|$ column gives the number of parameters in the network as a multiple of the ‘base’ 128-unit model.

longer an upper bound on performance because, for example, updating once on a sequence of length 10 with the true gradient may yield slower learning than updating twice on two consecutive sequences of length 5, with truncation.

In these experiments we examine SnAp performance for multiple sparsity levels and recurrent architectures including Vanilla RNNs, GRU, and LSTM. Table 3 includes the architectural details. The sparsity pattern is again chosen uniformly at random. As a result, comparison between sparsity levels is discouraged. For each configuration we sweep over learning rates in $\{10^{-3}, 10^{-3.5}, 10^{-4}\}$ and compare average performance over three seeds with the best chosen learning rate (all methods performed best with learning rate 10^{-3}). The minibatch size was 16. We train with either full unrolls or truncation with $T = 1$. This means that the RTRL approximations update the network weights at every timestep and persist a stale Jacobian (see section 2.2).

Fully online training One striking observation is that Truncated BPTT completely fails to learn long-term structure in the fully online ($T = 1$) regime. Interestingly, the SnAp methods perform *better* with more frequent updates. Compare solid versus dotted lines of the same color in Figure 5. Fully online SnAp-2 and SnAp-3 mostly outperform or match BPTT for training LSTM and GRU architectures despite the “staleness” noted in Section 2.2. We attribute this to the hypothesis advanced in the RTRL literature that Jacobian staleness can be mitigated with small learning rates but leave a more thorough investigation of this phenomenon to future work.

Bias versus computational expense For SnAp there is a tradeoff between the biasedness of the approximation and the computational costs of the algorithm. We see that correspondingly, SnAp-1 is outperformed by SnAp-2, which is in turn outperformed by SnAp-3 in the Copy experiments. The RFLO baseline is even more biased than SnAp-1, but both methods have comparable costs. SnAp-1 significantly outperforms RFLO in all of our experiments.

Empirical FLOPs requirements Here we augment the asymptotic cost calculations from Table 1 with empirical measurements of the FLOPs, broken out by architecture and sparsity level in Table 3. Gating architectures require a high degree of parameter sparsity in order to keep a commensurate amount of of Jacobian sparsity due to the increase

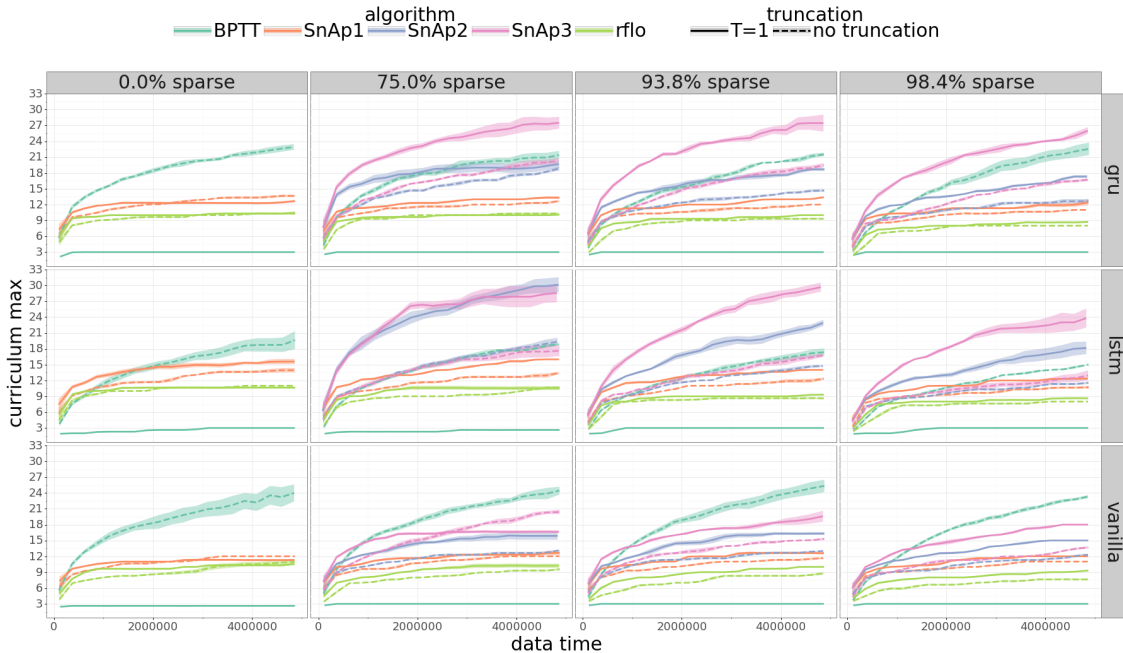


Figure 5: Copy task results by sparsity and architecture.

in density brought about by composing linear maps with different sparsity patterns (see section 3.3).

For instance, the 75% sparse GRU considered in the experiments from Section 5.1.2 lead to SnAp-2 parameter Jacobian that is only 70.88% sparse. With SnAp-3 it becomes much less sparse – only 50%. This may partly explain why SnAp performs best compared to BPTT in the LSTM case (Figure 5), though it still significantly outperforms BPTT in the high sparsity regime when SnAp-2 becomes practical. Also, LSTM is twice as costly to train with RTRL-like algorithms because it has two components to its state, requiring the maintenance of twice as many jacobians and the performance of twice as many jacobian multiplications (Equations 3/5). For a 75% sparse LSTM, the SnAp-2 Jacobian is much denser at 38.5% sparsity and SnAp-3 has essentially reached full density (so it is as costly as RTRL).

Figure 5 also shows that for Vanilla RNNs, increasing n improves performance, but SnAp does not outperform BPTT with this architecture. In summary, Increasing n improves performance but costs more FLOPs.

Architecture	Vanilla			GRU			LSTM		
Number of Units	128	256	512	128	256	512	128	256	512
Param. Sparsity	75.0%	93.8%	98.4%	75%	93.8%	98.4%	75.0%	93.8%	98.4%
SnAp-2 J Sparsity	83.0%	95.6%	98.9%	70.9%	91.1%	97.8%	38.5%	79.9%	95.1%
SnAp-3 J Sparsity	33.3%	59.2%	92.8%	50.0%	52.5%	71.6%	2.4%	5.9%	38.7%
SnAp-1 vs BPTT	1x	1x	1x	1x	1x	1x	2x	2x	2x
SnAp-2 vs BPTT	349x	90.4x	22.1x	597x	183x	44.8x	2518x	824.8x	200.1x
SnAp-3 vs BPTT	1365x	835.8x	147.5x	1024x	972x	582x	3996x	3855x	2513x
SnAp-2 vs RTRL	0.17x	0.044x	0.011x	0.291x	0.089x	0.022x	0.615x	0.201x	0.049x

Table 3: Empirical computational costs of SnAp, determined by the sparsity level in the Jacobians. The “X vs BPTT” rows express the FLOPS requirements of X as a multiple of BPTT training FLOPs. The “SnAp-2 vs RTRL” row shows the FLOPS requirements of SnAp-2 as a multiple of those required by optimized Sparse RTRL (section 3.2). Lower is better for all of these entries.

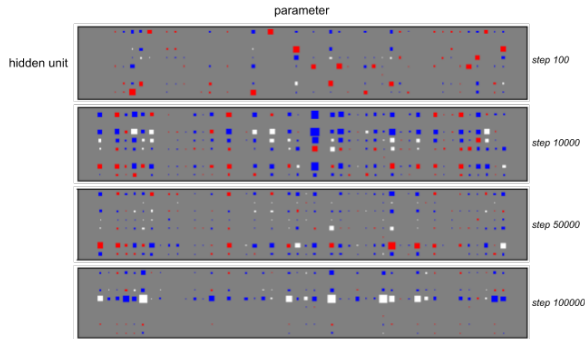


Figure 6: Influence matrix for 75% sparse GRU with 8 units after processing a full sequence with 35 timesteps (target length 16), at various points during training (“step” corresponds to training step, not e.g. the step within a sequence). This Hinton-diagram shows the magnitude of an entry with the size of a square. Grey entries are near zero. Entries filled in with red are those included by SnAp-1. Blue entries are those included by SnAp-2, and white ones are ignored by both approximations.

Training Step	SnAp-1	SnAp-2
100	1.0E-2 (73%)	4.0E-3 (97%)
5k	2.3E-1 (22%)	2.6E-1 (78%)
10k	1.1E-1 (23%)	1.2E-1 (85%)
50k	3.3E-1 (34%)	2.5E-1 (87%)
100k	2.4E-1 (6%)	6.5E-1 (51%)

Table 4: Approximation Quality of SnAp-1 and SnAp-2. Average magnitudes in the influence matrix versus whether or not they are kept by an approximate method. The “SnAp-1” and “SnAp-2” columns show the average magnitude of entries kept by the SnAp-1 and SnAp-2 approximations respectively. In parentheses is the sum of the magnitudes of entries in this category divided by the sum of all entry magnitudes in the influence matrix.

5.3 Analysis of the bias introduced by SnAp

Finally, we examine the empirical magnitudes of entries which are nonzero in the true, unapproximated influence matrix but set to zero by SnAp. For the benefit of visualization we train a small network on a non-curriculum variant of the Copy-task with target sequences fixed in length to 16 timesteps. This enables us to measure and display the bias of SnAp.

This particular run is a 8-unit GRU with 75% sparsity. The influence matrix considered is the final value after processing an entire sequence, which has 35 elements including the observation, target, and start/end flags. The network is optimized with full (untruncated) BPTT. We find (Table 4) that at the beginning of training the influence entries ignored by SnAp are small in magnitude compared to those kept, even after the influence has had many RNN iterations to fill in.

This analysis complements the experimental results concerning how useful the approximate gradients are for learning; instead it shows where — and by how much — the sparse approximation to the influence differs from the true accumulated influence. Interestingly, despite the strong task performance of SnAp, the magnitude of ignored entries in the influence matrix is not always small (see Figure 6). The accuracy, as measured by such magnitudes, trends downward over the course of training. We speculate that designing methods to temper the increased bias arising later in training may be beneficial but leave this to future work.

6 Conclusion

We have shown how sparse operations can make a form of RTRL efficient, especially when replacing dense parameter Jacobians with approximate sparse ones. We introduced SnAp-1, an efficient RTRL approximation which outperforms comparably-expensive alternatives on a popular language-modeling benchmark. We also developed higher orders of SnAp including SnAp-2 and SnAp-3, approximations tailor-made for sparse RNNs which can be efficient in the regime of high parameter sparsity, and showed that they can learn temporal structure considerably faster than even full BPTT.

Our results suggests that training very large, sparse RNNs could be a promising path toward more powerful sequence models trained on arbitrarily long sequences. This may prove useful for modelling whole documents such as articles or even books, or reinforcement learning agents which learn over an entire lifetime rather than the brief episodes which are common today. A few obstacles stand in the way of scaling up our methods further:

- The need for a high-performing sparse training strategy that does not require dense gradient information.
- Sparsity support in both software and hardware that enables better realization of the theoretical efficiency gains of sparse operations.

It may also be fruitful to further develop our methods for hybrid models combining recurrence and attention [7] or even feedforward architectures with tied weights [21] [8].

Acknowledgements

We wish to thank Max Jaderberg, Siddhant Jayakumar, Jack Rae, Greg Wayne, Daan Wierstra, Tim Harley, James Martens, Corentin Tallec, Danilo Rezende, Charles Blundell, Tim Lillicrap, Peter Humphreys, Vlad Firoiu, Matthew Johnson, Jeffrey De Fauw, and Maneesh Sahani for stimulating discussions. We also thank the Jax [3] and Haiku [17] teams for creating infrastructure that made this very fun to implement.

References

- [1] Dario Amodei, Sundaram Ananthanarayanan, Rishita Anubhai, Jingliang Bai, Eric Battenberg, Carl Case, Jared Casper, Bryan Catanzaro, Qiang Cheng, Guoliang Chen, and et al. Deep speech 2: End-to-end speech recognition in english and mandarin. In *Proceedings of the 33rd International Conference on International Conference on Machine Learning - Volume 48*, ICML 16, page 173–182. JMLR.org, 2016.
- [2] Frederik Benzing, Marcelo Matheus Gauy, Asier Mujika, Anders Martinsson, and Angelika Steger. Optimal kronecker-sum approximation of real time recurrent learning. In Kamalika Chaudhuri and Ruslan Salakhutdinov, editors, *Proceedings of the 36th International Conference on Machine Learning, ICML 2019, 9-15 June 2019, Long Beach, California, USA*, volume 97 of *Proceedings of Machine Learning Research*, pages 604–613. PMLR, 2019. URL <http://proceedings.mlr.press/v97/benzing19a.html>.
- [3] James Bradbury, Roy Frostig, Peter Hawkins, Matthew James Johnson, Chris Leary, Dougal Maclaurin, and Skye Wanderman-Milne. JAX: composable transformations of Python+NumPy programs, 2018. URL <http://github.com/google/jax>.
- [4] Mia Xu Chen, Orhan Firat, Ankur Bapna, Melvin Johnson, Wolfgang Macherey, George Foster, Llion Jones, Mike Schuster, Noam Shazeer, Niki Parmar, Ashish Vaswani, Jakob Uszkoreit, Lukasz Kaiser, Zhifeng Chen, Yonghui Wu, and Macduff Hughes. The best of both worlds: Combining recent advances in neural machine translation. In *Proceedings of the 56th*

- Annual Meeting of the Association for Computational Linguistics (Volume 1: Long Papers)*, pages 76–86, Melbourne, Australia, July 2018. Association for Computational Linguistics. doi: 10.18653/v1/P18-1008. URL <https://www.aclweb.org/anthology/P18-1008>.
- [5] Kyunghyun Cho, Bart van Merriënboer, Caglar Gulcehre, Dzmitry Bahdanau, Fethi Bougares, Holger Schwenk, and Yoshua Bengio. Learning phrase representations using RNN encoder–decoder for statistical machine translation. In *Proceedings of the 2014 Conference on Empirical Methods in Natural Language Processing (EMNLP)*, pages 1724–1734, Doha, Qatar, October 2014. Association for Computational Linguistics. doi: 10.3115/v1/D14-1179. URL <https://www.aclweb.org/anthology/D14-1179>.
- [6] Tim Cooijmans and James Martens. On the variance of unbiased online recurrent optimization. *CoRR*, abs/1902.02405, 2019. URL <http://arxiv.org/abs/1902.02405>.
- [7] Zihang Dai, Zhilin Yang, Yiming Yang, Jaime Carbonell, Quoc Le, and Ruslan Salakhutdinov. Transformer-XL: Attentive language models beyond a fixed-length context. In *Proceedings of the 57th Annual Meeting of the Association for Computational Linguistics*, pages 2978–2988, Florence, Italy, July 2019. Association for Computational Linguistics. doi: 10.18653/v1/P19-1285. URL <https://www.aclweb.org/anthology/P19-1285>.
- [8] Mostafa Dehghani, Stephan Gouws, Oriol Vinyals, Jakob Uszkoreit, and Lukasz Kaiser. Universal transformers. *CoRR*, abs/1807.03819, 2018. URL <http://arxiv.org/abs/1807.03819>.
- [9] Erich Elsen, Marat Dukhan, Trevor Gale, and Karen Simonyan. Fast Sparse ConvNets. *ArXiv*, 2019. URL <https://arxiv.org/abs/1911.09723>.
- [10] Jesse Engel. Optimizing rnns with differentiable graphs. URL https://svail.github.io/diff_graphs/. Accessed: 2020-06-02.
- [11] Lasse Espeholt, Hubert Soyer, Remi Munos, Karen Simonyan, Volodymir Mnih, Tom Ward, Yotam Doron, Vlad Firoiu, Tim Harley, Iain Dunning, et al. IMPALA: Scalable Distributed Deep-RL with Importance Weighted Actor-Learner Architectures. In *Proceedings of the International Conference on Machine Learning (ICML)*, 2018.
- [12] Utku Evci, Trevor Gale, Jacob Menick, Pablo Samuel Castro, and Erich Elsen. Rigging the Lottery: Making All Tickets Winners, 2019.
- [13] Jonathan Frankle and Michael Carbin. The lottery ticket hypothesis: Finding sparse, trainable neural networks. In *7th International Conference on Learning Representations, ICLR 2019, New Orleans, LA, USA, May 6-9, 2019*, 2019. URL <https://openreview.net/forum?id=rJl-b3RcF7>.
- [14] Alex Graves, Greg Wayne, Malcolm Reynolds, Tim Harley, Ivo Danihelka, Agnieszka Grabska-Barwińska, Sergio Gómez Colmenarejo, Edward Grefenstette, Tiago Ramalho, John Agapiou, Adrià Puigdomènech Badia, Karl Moritz Hermann, Yori Zwols, Georg Ostrovski, Adam Cain, Helen King, Christopher Summerfield, Phil Blunsom, Koray Kavukcuoglu, and Demis Hassabis. Hybrid computing using a neural network with dynamic external memory. *Nature*, 538(7626):471–476, 2016. doi: 10.1038/nature20101. URL <https://doi.org/10.1038/nature20101>.
- [15] Andreas Griewank and Andrea Walther. Algorithm 799: Revolve: An implementation of checkpointing for the reverse or adjoint mode of computational differentiation. *ACM Trans. Math. Softw.*, 26(1):19–45, March 2000. ISSN 0098-3500. doi: 10.1145/347837.347846. URL <https://doi.org/10.1145/347837.347846>.
- [16] Audrunas Gruslys, Remi Munos, Ivo Danihelka, Marc Lanctot, and Alex Graves. Memory-efficient backpropagation through time. In D. D. Lee, M. Sugiyama, U. V. Luxburg, I. Guyon, and R. Garnett, editors, *Advances in Neural Information Processing Systems 29*, pages 4125–4133. Curran Associates, Inc., 2016. URL <http://papers.nips.cc/paper/6221-memory-efficient-backpropagation-through-time.pdf>.
- [17] Tom Hennigan, Trevor Cai, Tamara Norman, and Igor Babuschkin. Haiku: Sonnet for JAX, 2020. URL <http://github.com/deepmind/dm-haiku>.
- [18] Sepp Hochreiter and Jürgen Schmidhuber. Long short-term memory. *Neural Comput.*, 9(8):1735–1780, November 1997. ISSN 0899-7667. doi: 10.1162/neco.1997.9.8.1735. URL <http://dx.doi.org/10.1162/neco.1997.9.8.1735>.

- [19] Nal Kalchbrenner, Erich Elsen, Karen Simonyan, Seb Noury, Norman Casagrande, Edward Lockhart, Florian Stimberg, Aäron van den Oord, Sander Dieleman, and Koray Kavukcuoglu. Efficient Neural Audio Synthesis. In *Proceedings of the 35th International Conference on Machine Learning, ICML 2018, Stockholm*, Stockholm, Sweden, July 10-15, 2018, pages 2415–2424, 2018.
- [20] Diederik P. Kingma and Jimmy Ba. Adam: A method for stochastic optimization, 2014. URL <http://arxiv.org/abs/1412.6980>. cite arxiv:1412.6980Comment: Published as a conference paper at the 3rd International Conference for Learning Representations, San Diego, 2015.
- [21] Zhenzhong Lan, Mingda Chen, Sebastian Goodman, Kevin Gimpel, Piyush Sharma, Radu Soricut, Google Research, and Mailton de Carvalho. Albert: A lite bert for self-supervised learning of language representations. 10 2019.
- [22] Stephen Merity, Caiming Xiong, James Bradbury, and Richard Socher. Pointer sentinel mixture models. In *5th International Conference on Learning Representations, ICLR 2017, Toulon, France, April 24-26, 2017, Conference Track Proceedings*. OpenReview.net, 2017. URL <https://openreview.net/forum?id=Byj72udxe>.
- [23] Asier Mujika, Florian Meier, and Angelika Steger. Approximating real-time recurrent learning with random kronecker factors. In S. Bengio, H. Wallach, H. Larochelle, K. Grauman, N. Cesa-Bianchi, and R. Garnett, editors, *Advances in Neural Information Processing Systems 31*, pages 6594–6603. Curran Associates, Inc., 2018. URL <http://papers.nips.cc/paper/7894-approximating-real-time-recurrent-learning-with-random-kronecker-factors.pdf>.
- [24] James M Murray. Local online learning in recurrent networks with random feedback. *eLife*, 8:e43299, may 2019. ISSN 2050-084X. doi: 10.7554/eLife.43299. URL <https://doi.org/10.7554/eLife.43299>.
- [25] Sharan Narang, Gregory F. Diamos, Shubho Sengupta, and Erich Elsen. Exploring sparsity in recurrent neural networks. In *International Conference on Learning Representations*, 2017.
- [26] Jack W Rae, Jonathan J Hunt, Tim Harley, Ivo Danihelka, Andrew Senior, Greg Wayne, Alex Graves, and Timothy P Lillicrap. Scaling memory-augmented neural networks with sparse reads and writes. In *Proceedings of the 30th International Conference on Neural Information Processing Systems, NIPS’16*, page 3628–3636, Red Hook, NY, USA, 2016. Curran Associates Inc. ISBN 9781510838819.
- [27] Nikko Ström. Sparse connection and pruning in large dynamic artificial neural networks. In *EUROSPEECH*, 1997.
- [28] Corentin Tallec and Yann Ollivier. Unbiased online recurrent optimization. In *International Conference on Learning Representations*, 2018. URL <https://openreview.net/forum?id=rJQDjk-0b>.
- [29] R. J. Williams and D. Zipser. A learning algorithm for continually running fully recurrent neural networks. *Neural Computation*, 1(2):270–280, June 1989. ISSN 0899-7667. doi: 10.1162/neco.1989.1.2.270.
- [30] Ronald J. Williams and Jing Peng. An efficient gradient-based algorithm for on-line training of recurrent network trajectories. *Neural Computation*, 2:490–501, 1990.
- [31] Michael Zhu and Suyog Gupta. To Prune, or Not to Prune: Exploring the Efficacy of Pruning for Model Compression. In *International Conference on Learning Representations Workshop*, 2018.